Intra- and Intermolecular Effects on ^{1}H Chemical Shifts in a Silk Model Peptide Determined by High-Field Solid State ^{1}H NMR and Empirical Calculations

Yu Suzuki,[†] Rui Takahashi,[†] Tadashi Shimizu,[‡] Masataka Tansho,[‡] Kazuo Yamauchi,[†] Mike P. Williamson,[§] and Tetsuo Asakura*[,†]

Department of Biotechnology, Tokyo University of Agriculture and Technology, 2-24-16, Nakacho, Koganei, Tokyo 184-8588, Japan, National Institute for Material Science, 3-13 Sakura, Tsukuba, Ibaraki 305-0003, Japan, Department of Molecular Biology and Biotechnology, University of Sheffield, Firth Court, Western Bank Sheffield S10 2TN, U.K.

Received: April 2, 2009; Revised Manuscript Received: May 17, 2009

A combination of solid state ^{1}H NMR chemical shift measurements and empirical chemical shift calculations has been used to interpret ^{1}H solid state chemical shifts of a model peptide $(Ala\text{-}Gly)_{15}$ for the crystalline domain of *Bombyx mori* silk fibroin in silk I and silk II structures, including a treatment of both intra- and intermolecular arrangements. Silk I and silk II are the structures of silk fibroin before and after spinning, respectively. Two peaks with equal intensity were observed for the amide protons of $(AG)_{15}$ in silk I, whereas only one broad peak was observed for silk II, reflecting a difference of 1.1 ppm in Ala H^N shift between silk I and silk II, but a difference of only 0.2 ppm in Gly H^N shift. Chemical shift calculations predicted chemical shifts that are in good agreement with the experimental observations and showed that the origin of these chemical shift differences was predominantly the magnetic anisotropy effect from the C═O bond that hydrogen bonds with H^N, which has a more favorable geometry for Ala H^N in silk II than for the other H^N. This result shows that we could distinguish between proton chemical shift effects arising from intermolecular interactions and those from intramolecular interactions by combining observation of the solid state ^{1}H NMR chemical shift and empirical chemical shift calculation.

Introduction

The ^{1}H chemical shift is a fundamental and informative NMR parameter, but unlike other nuclei such as ^{13}C and ^{15}N, it has been little used for protein structure analysis by solid state NMR because of its low resolution originating from the strong ^{1}H−^{1}H dipole interaction. Recently, ^{1}H NMR chemical shifts of peptides and proteins in the solid state have been observed with CRAMPS (Combined Rotations And Multiple-Pulse Sequence),[1−3] high-speed MAS,[4,5] and ultrahigh-field NMR,[6−8] including the observation of amide protons, which are broadened more than other protons because of residual dipolar coupling to the ^{14}N quadrupolar nuclei. ^{1}H chemical shifts are particularly interesting because they have a strong dependence on intermolecular interactions, as compared to ^{13}C and ^{15}N, in which most of the chemical shift effects are intramolecular.[9,10] We and other groups have analyzed the relationship between the ^{1}H chemical shift and local spatial structure in peptides, polypeptides, and proteins on the basis of calculations of the ring current effect, magnetic anisotropy effect and electric field effect, and so on.[11−15] This relationship has been used for structure calculation[16−18] and validation,[19] and shows great promise for de novo calculation of protein structures.[20,21] In the solid state, ^{1}H NMR chemical shifts should give information on the intermolecular chain arrangement as well as the conformation. However, to date there have been only limited reports on the intermolecular chain arrangement of peptides, polypeptides, and proteins using ^{1}H solid state NMR chemical shifts.[4,7]

In this paper, a combination of solid-state ^{1}H NMR chemical shift measurements and empirical chemical shift calculations has been used to interpret the ^{1}H solid state chemical shifts of the model peptide $(Ala\text{-}Gly)_{15}$. This sequence is found in the crystalline domain of *Bombyx mori* (domesticated silkworm) silk fibroin and adopts two alternative regular structures: silk I, which is a crystalline form found within the spinneret before spinning, and silk II, which is the more well-known silk fiber structure. The silk I structure has been shown to consist of a repeated structure of type II β-turns, stabilized by 4 → 1 intramolecular hydrogen bonds.[22−26] The planar sheets are held together by intermolecular hydrogen bonds, involving the central amide bond of the β-turn, perpendicular to the intramolecular interactions. By contrast, silk II has an antiparallel β-sheet structure with intermolecular hydrogen bonding. This structure constitutes approximately 70% of silk fiber, the rest being distorted β-turn or random coil conformation.[27−34] Thus, these silk I and silk II structures are a good system to discuss the relationship between ^{1}H solid state NMR chemical shifts and the intermolecular local structure. In addition, there are many papers on applications of silk to biomaterials in recent years.[35] The physical properties of silk depend on its heterogeneous structure, and therefore, it is particularly challenging to obtain structural information. Solid state NMR has proved to be a powerful method for such materials. See, for example, the references above and also refs 36−38.

Materials and Methods

Materials. The alanine and glycine alternating copolypeptide $(Ala\text{-}Gly)_{15}$ was synthesized by the Fmoc solid-phase method

* To whom correspondence should be addressed. E-mail: asakura@cc.tuat.ac.jp.
[†] Tokyo University of Agriculture and Technology.
[‡] National Institute for Material Science.
[§] University of Sheffield.

10.1021/jp903020p CCC: $40.75
Published on Web 07/01/2009

on a Pioneer Peptides Synthesis System (Applied Biosystems Ltd., Warrington, U.K.). The peptide was assembled on Fmoc-Gly-PEG-PS resin (0.19 mmol/g), and the coupling of Fmoc amino acids was performed by HATU (2-(1H-7-Azabenzotriazol-1-yl)--1,1,3,3-tetramethyl uranium hexafluorophosphate Methanaminium). After completing the synthesis, peptides were released from the resin by treatment with a mixture of trifluoroacetic acid, phenol, triisopropylsilane, and water (88:5:2:5 v/v). The purity of $(Ala-Gly)_{15}$ prepared here was checked by ^{13}C solution NMR of the peptide in 60% LiSCN solution[39] and estimated as more than 90%. The peptide was converted to silk I using a widely accepted method:[40,41] the crude peptide was dissolved in 9 M lithium bromide and then dialyzed (molecular weight cutoff = 1000 Da) against distilled water for three days at 4 °C. The naturally precipitated peptide after dialysis was collected and lyophilized. To transform silk I into silk II, the peptide was dissolved in formic acid and then dried at ambient temperature.[28] The structures were confirmed by IR and ^{13}C CP/MAS NMR as reported previously.[25,28]

High-Field Solid-State NMR Measurements. All of the solid-state NMR spectra were recorded on an ECA 930 spectrometer operating at a proton frequency of 929.81 MHz installed at the National Institute for Material Science, Tsukuba, Japan. For ^{1}H 1D measurements, a 45° pulse (2 μs) was used for spectral acquisition, together with a repetition time of 5 s, spinning frequency of 20 kHz, and 32 transients. The ^{1}H solid-state chemical shift was referenced to the peak of silicon rubber inserted in the rotor and set to 0.12 ppm from TMS. An exponential window function of 20 Hz was used. For 2D ^{1}H−^{15}N HETCOR (HETeronuclear CORrelation) measurements, the 90° pulse width was 3.6 μs for ^{1}H, and the repetition time was 4 s. The spinning frequency was set to 10 kHz. The PMLG pulse sequence,[42] a variant of the Lee−Goldburg method,[43] was used for homonuclear decoupling of ^{1}H, and the ^{1}H chemical shift was calculated with a scaling factor of 0.573. ^{15}N chemical shifts were calibrated indirectly from external $^{15}NH_4Cl$ at 18.0 ppm. Approximately 20 mg of the peptide $(Ala-Gly)_{15}$ was contained in a zirconium dioxide, o.d. 4 mm rotor for both measurements.

Empirical Chemical Shift Calculation. Empirical ^{1}H chemical shift calculations were performed with the program SHIFTCALC developed by Williamson and Asakura.[11,12] Secondary (structure-dependent) chemical shifts are calculated as a sum of ring-current shifts, shifts from the electric field arising from polar atoms, and shifts arising from the magnetic anisotropy of the C=O and C−N bonds. Twelve chains of $(Ala-Gly)_6$ in a repeated type II β-turn structure[22] were arranged for the ^{1}H chemical shift calculation of the silk I model (a single chain and 12 chains are shown as Figure 1A). Sixteen chains of $(Ala-Gly)_3$ in antiparallel β-sheet form[34] were arranged for the silk II model (2 chains and 16 chains are shown as Figure 1B).

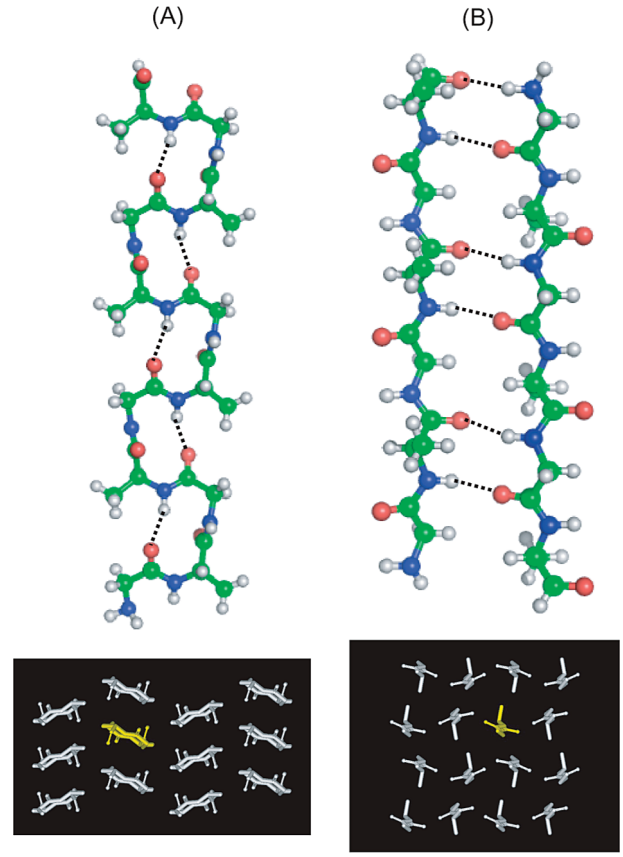

Figure 1. The upper structures are silk I (A: repeated β-turn type II structure[25]) and silk II (B: antiparallel β-sheet structure[34]). The lower chain arrangements were used for the ^{1}H chemical shift calculation. The ^{1}H chemical shift data of the chains represented as sticks and balls are listed in Table 1.

TABLE 1: Observed and Calculated ^{1}H Chemical Shifts of Ala-Gly Repeat Peptides in Silk I and Silk II Forms (±0.1 ppm)

	Ala			Gly		
	H^N	H^α	H^β	H^N	$H^{\alpha1}$	$H^{\alpha2}$
			Observed			
silk I	7.9	4.1[a]	1.4	9.0	3.5[a]	
silk II	9.0	4.9[a]	1.1	9.2	3.6[a]	
			Calculated			
silk I	8.08	4.14	1.65	8.56	3.74	3.36
silk II	9.14	4.28	1.24	8.44	3.45	4.20

[a] Experimental data of Kishi et al.,[1] obtained from HETCOR spectra. From 1D spectra, only a single overlapped signal can be observed, which in our spectra is also overlapped with the water resonance.

Results and Discussion

^{1}H Solid-State NMR Spectra of $(Ala-Gly)_{15}$ in Silk I and Silk II Forms. Figure 2A illustrates the ^{1}H solid-state NMR spectra of $(Ala-Gly)_{15}$ in silk I (solid line) and silk II (dotted line) forms. The sharp peak at 0.12 ppm is from the silicon rubber used as the internal chemical shift reference, and the peak at around 3.8 ppm was assigned to water molecules in the samples. Three spectral regions in both spectra can be resolved: the amide region (7.9−9.0 ppm), the CH and CH_2 region, and the Ala CH_3 region to higher field. Although determination of the H^N chemical shift is, in general, not easy in the ^{1}H CRAMPS experiment because of the line broadening due to residual dipolar coupling between quadrupolar ^{14}N nuclei and the amide proton, the amide region could be observed easily here because of the increased resolution arising from the high-field magnet.

Amide Proton Chemical Shifts. In the H^N region of the 1D spectrum, two peaks were observed at 7.9 and 9.0 ppm in the silk I spectrum and a single peak at approximately 9.1 ppm in the silk II spectrum. Thus, the H^N peaks of the Ala and Gly residues were separated by 1.1 ppm in silk I, but overlapped in silk II. Peak assignments were made using ^{1}H−^{15}N HETCOR spectra on ^{15}N single-labeled Ala-Gly repeated silk model peptides (data not shown) and on *B. mori* silk fibroin,[44] which match well to the shifts observed in ^{1}H−^{15}N HETCOR spectra of an unlabeled $(AG)_{15}$ peptide (Figure 3) in both silk I and

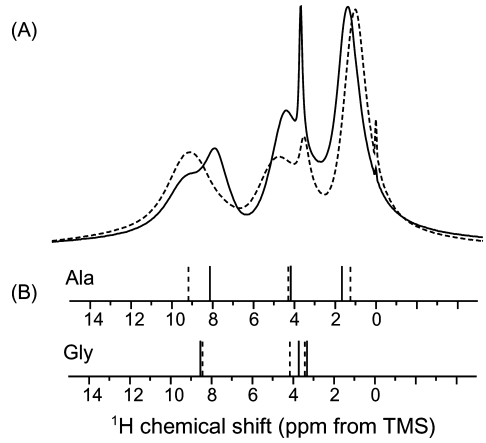

Figure 2. (A) ^{1}H MAS NMR spectra of $(AG)_{15}$ in silk I (solid line) and silk II (dotted line) forms. (B) Stick spectra of ^{1}H chemical shifts calculated by empirical chemical shift calculation are also shown.

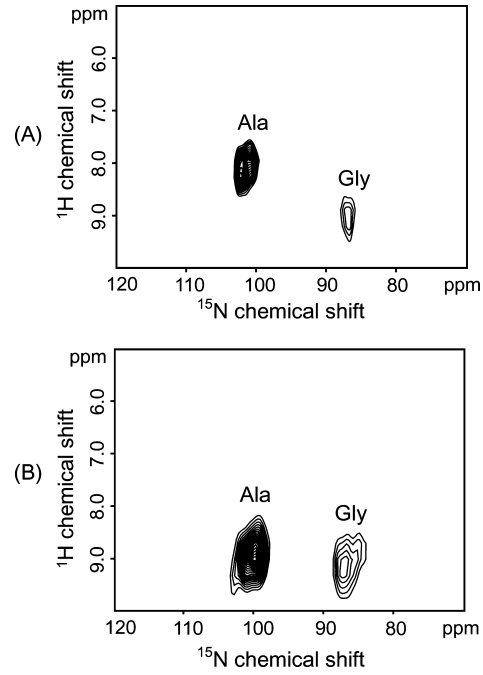

Figure 3. 2D ^{1}H$-^{15}$N HETCOR NMR spectra of $(AG)_{15}$ in silk I (A) and silk II(B) forms.

silk II conformations. These spectra show that the Ala and Gly signals in silk II actually resonate at 9.0 and 9.2 ppm, respectively.

The H^N chemical shifts were also calculated for the silk I and silk II models using the program SHIFTCALC, which is paramaterized empirically using shift values observed for proteins in solution. The benefit of using this type of calculation (by comparison, for example, to density functional theory (DFT) methods) is that it is easy to analyze which structural features cause different chemical shift effects. The calculated chemical shifts are summarized in Table 1 and are also shown as stick spectra in Figure 2B. The Ala H^N chemical shifts showed a large difference between silk I and silk II forms, whereas the chemical shift difference for Gly between the two forms was negligibly small. Thus, the ^{1}H chemical shift features for the Ala and Gly H^Ns were reproduced well. In particular, the assignments predicted from the calculation match the results from HETCOR. It is therefore possible to use the calculations to understand the differences in experimental shifts.

TABLE 2: Amide Proton Chemical Shift Contribution from Electric Field Effect (σ^E) and Magnetic Anisotropy Effect from C═O ($\sigma^{C=O}$) and C−N (σ^{C-N}) Bonds (ppm)

	Ala		Gly	
	silk I	silk II	silk I	silk II
σ^E	0.30	0.36	0.29	0.17
$\sigma^{C=O}$	0.08	0.73	0.17	0.10
σ^{C-N}	−0.34	0.01	−0.03	0.04

TABLE 3: Calculated ^{1}H Chemical Shifts of Ala-Gly Repeat Peptides in Silk I and Silk II Forms[a]

	silk I		silk II	
	single chain	multiple chains	single chain	multiple chains
		Ala		
H^N	8.17	8.08	8.33	9.14
H^α	4.18	4.14	4.29	4.28
H^β	1.46	1.65	1.33	1.24
		Gly		
H^N	8.50	8.56	8.39	8.44
$H^{\alpha1}$	3.90	3.74	3.79	3.45
$H^{\alpha2}$	3.86	3.36	4.31	4.20

[a] Interpretation of "single chain" and "multiple chains" was described in the text.

The spectra show that the Ala H^N chemical shifts have a large difference between silk I and silk II forms, whereas those of Gly are very small. The chemical shift difference for Ala H^N reflects the well-known tendency that H^N protons in β sheet tend to be observed at lower field and in α helix tend to be observed at higher field.[45] However, the Gly H^N shifts do not display this behavior. The origin of the chemical shift difference was therefore analyzed in more detail. The ^{1}H chemical shift calculations represent the chemical shift as a sum of ring-current effects, effects from the electric field arising from polar atoms, and effects arising from the magnetic anisotropy of the C═O and C−N bonds. In this study, ring-current effects are zero because there are no aromatic rings in the peptide. The contributions from the electric field and magnetic anisotropies of the C═O and C−N bonds to the amide protons are listed in Table 2. The calculations show that all three contributions are significant, with little change for Gly between silk I and silk II, but major changes in Ala for the bond magnetic anisotropy effects. However, this analysis offers little insight into the structural origins of the shifts.

The intermolecular effects on H^N chemical shifts were therefore analyzed by comparing calculations carried out using a single isolated chain with calculations on multiple chains surrounding the relevant protons. The calculated results are collected in Table 3. It is noteworthy that the chemical shift difference between Ala H^N in a single chain and in multiple chains in silk II was 0.81 ppm, whereas those of other H^Ns were less than 0.1 ppm. The small difference for Ala H^N in silk I could be expected because it forms exclusively intramolecular hydrogen bonds (Figure 1), as could the larger difference of Ala H^N in silk II due to its intermolecular hydrogen bonding. However, it was less expected that the differences for Gly H^N in both silk I and silk II were very small, despite the fact that they have intermolecular hydrogen bonding in both structures.

To analyze further the origin of the chemical shift difference between silk I and silk II, the calculated results obtained from multiple chains were examined in detail. The overall magnetic anisotropy and electric field effects are calculated as the scalar sum of the anisotropies of individual bonds and the electric field

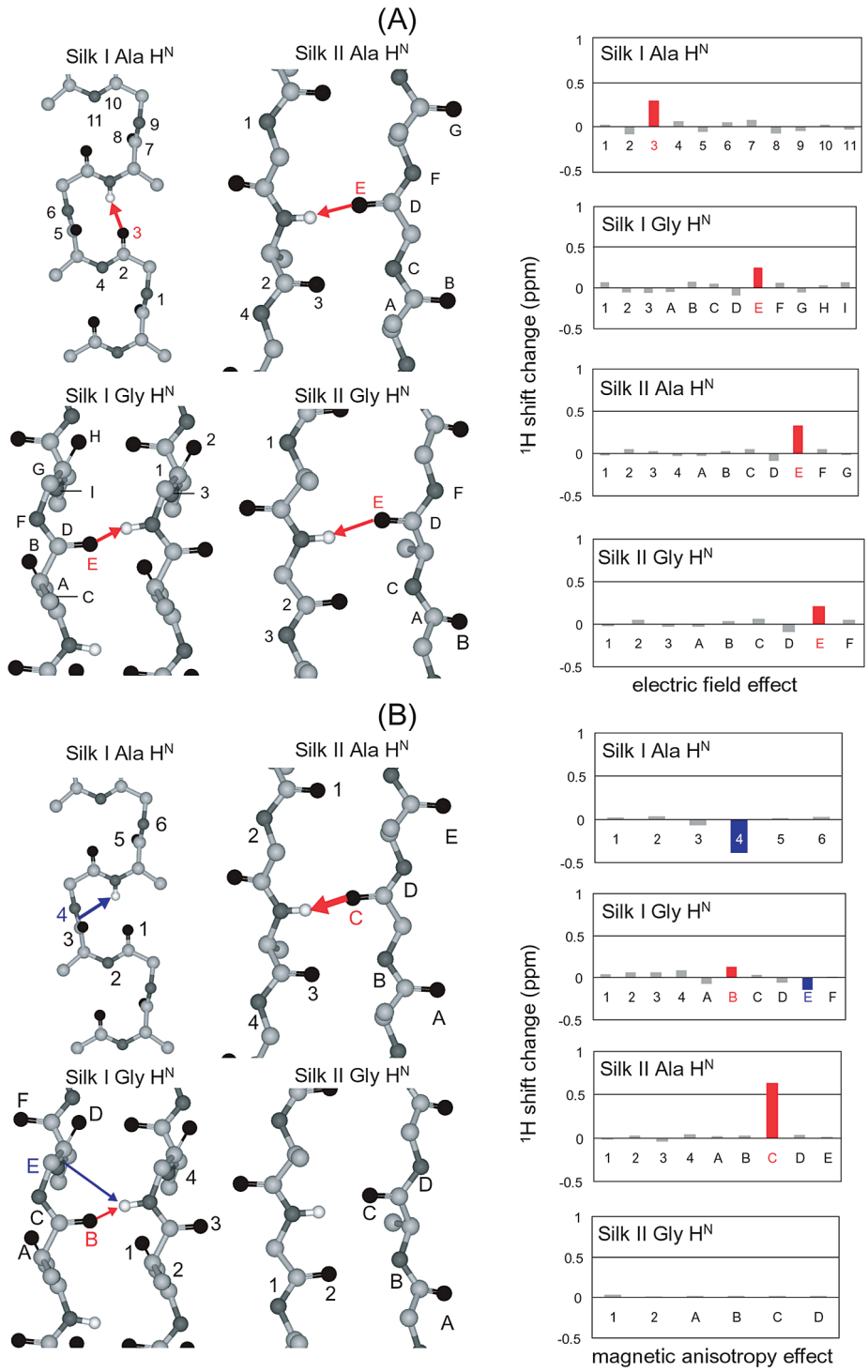

Figure 4. (A) The contribution of the electric field effect from each neighboring O, C, and N nucleus to the Ala H^N and Gly H^N shift. (B) The contribution from the magnetic anisotropy effect of each neighboring C═O and C−N bond to the Ala H^N and Gly H^N shift. Numbers denote intramolecular effects, and letters denote intermolecular effects. The arrows represent calculated shielding effects over 0.1 ppm. Downfield and upfield shielding effects are represented as red and blue, respectively.

effects produced by neighboring charged atoms. To characterize the origin of these chemical shifts in detail, each contribution of the electric field and bond anisotropy effects to the H^N chemical shift was examined. Figure 4A shows the electric field effect for each H^N from each polar atom. For all H^N, the dominant contribution is from the directly hydrogen bonding oxygen atom, and there are no significant differences between the different structures, in agreement with the small changes listed in Table 2. Figure 4B shows the bond magnetic anisotropy contribution for each H^N from each C═O and C−N bond. From this figure, it is clear that the large downfield shift for Ala H^N in silk II comes, as expected, from the C═O bond of the glycine on the neighboring strand to which it is hydrogen bonded. However, in silk I, the intramolecularly hydrogen bonded C═O contributes very little, and the largest (upfield) effect is from the C−N of the preceding amide, which is spatially close. For the Gly H^N, neither of the intermolecular hydrogen bonds in silk I or in silk II has any significant effect on the shift. Thus,

TABLE 4: The Angles (degree), θ and γ, Used for the Calculation, σ^{ani} in Eq 1[a]

	silk I		silk II	
angle	Ala	Gly	Ala	Gly
θ	49	54	87	57
γ	22	16	11	47

[a] The definitions of the angles were described in the text.

TABLE 5: The Geometry: Length (angstrom) and Angles (degree) for Hydrogen Bonds in Silk I and Silk II Forms

	Ala		Gly	
	silk I	silk II	silk I	silk II
N−H···O length	2.05	1.87	2.00	2.30
N−H···O angle	158.0	167.2	137.6	144.2

surprisingly, the directly hydrogen bonding carbonyl has a significant effect on the H^N shift only for silk II Ala.

This difference can be understood from eq 1 for the magnetic anisotropy effect,[46,47]

$$\sigma^{ani} = (1/3r^3)[\Delta\chi_1 1(1 - 3\cos^2\theta) + \Delta\chi_2(1 - 3\sin^2\theta\sin^2\gamma)] \quad (1)$$

where $\Delta\chi_1 = -11.0$ and $\Delta\chi_2 = -5.0$ for the C═O bond anisotropies as optimized in our previous study.[12]

The x axis is coincident with the bond axis, the y axis is the direction orthogonal to the peptide plane, and the z axis is then orthogonal to these two axes. θ is the angle between the y axis and the vector **r** from the center of the magnetic anisotropy (15% of the distance from O to C on the C═O bond) to the proton atom (distance r). γ is the angle between the projection of **r** in the xz plane and the x axis. The angles θ and γ between hydrogen bonding H^N and C═O bonds are listed in Table 4. The maximum shielding is obtained for a combination of $\theta = 0°$ and $\gamma = 90°$ (perpendicular to the C═O bond), and the maximum deshielding is calculated at the combination of $\theta = 90°$ and $\gamma = 0°$ (in line with the C═O bond). The angle θ of Ala H^N in silk II is the largest for any H^N, and in addition, γ is the smallest: in other words, this hydrogen bond is the closest to a linear C═O···H geometry, whereas the others are rather distorted. This is the reason why the Ala H^N in silk II resonates at a much lower field as compared with other H^Ns. Furthermore, the length of the hydrogen bond to Ala H^N in silk II is considerably shorter than those of other H^N, and the N−H···O angle of silk II is also closer to 180° than for other protons, as summarized in Table 5.

H^α and H^β Chemical Shifts. The H^α peaks of the Ala and Gly residues are overlapped and somewhat obscured by the water resonance and, thus, do not contain useful structural information.

The observed Ala H^β chemical shifts are in good agreement with those reported by Kishi et al.[1] The calculated chemical shift difference between silk I and silk II is 0.41 ppm, which is close to the observed difference (0.3 ppm). The H^β shift can be expected to contain packing information, since it is very close to the neighboring sheet. In agreement with this, the origin of the shift difference is the C−N bond anisotropy effect of the Gly residue in the opposite sheet. To investigate the sensitivity of the H^β shift to packing, the distance between the sheets in the molecular model was varied by between −0.4 and +1.0 Å in 0.2 Å steps, and chemical shifts were calculated. However, the change was fairly small in that even the 1.0 Å change produced only a 0.1 ppm shift change (data not shown). We conclude that it is difficult to obtain packing information from H^β at this ^{1}H NMR resolution, even though the main effect on its shift derives from the opposite sheet.

Comparison of ^{1}H and ^{13}C Values. In this paper, we have shown that ^{1}H shifts observed by solid state NMR, particularly H^N shifts, are useful for characterizing the strength of intermolecular hydrogen bonds. This information would more conventionally be investigated in the solid state using ^{13}C shifts. Therefore, we briefly discuss the application of ^{13}C shifts to this question.

Intermolecular effects on ^{13}C shifts, such as ring current and bond magnetic anisotropy effects, are the same size in parts per million for ^{13}C as they are for ^{1}H.[48] However, because the range of intramolecular effects on ^{13}C shifts is much larger than it is for ^{1}H (as demonstrated by the approximately 20-fold larger chemical shift range for ^{13}C) and because ^{13}C atoms are generally less surface-exposed than ^{1}H, intermolecular effects are much less important for ^{13}C in comparison to intramolecular effects. Thus, for example, the authors of the chemical shift prediction program SHIFTX quote hydrogen bonding as determining approximately 20% of the chemical shift range in their analysis for H^N but 0% for C′, Cα, or Cβ.[15] For this system, empirical correlations[49] suggest that the difference between silk I and silk II should be −1.1, +2.5, and −0.9 ppm for Ala Cα, Ala Cβ, and Gly Cα, respectively, on the basis of only conformational effects, as compared to experimental differences[1] of −2.0, +3.6, and −0.5 ppm. Since the root mean square error in the calculated shifts is ∼1 ppm for Cα and Cβ, the experimental shifts are reasonably well matched by the intramolecular conformational effects, without considering hydrogen bonds. The effect of hydrogen bonding is in each case ∼0.25 ppm.[45] For carbonyl shifts, predicted hydrogen bond effects are ∼0.4 ppm,[10] which are again much smaller than the conformational effects. Therefore, for C′, Cα, and Cβ, we conclude that hydrogen bonding makes only a small difference to the chemical shifts (and is within the uncertainty of the intramolecular effects) and that the ^{13}C shifts cannot be used to characterize hydrogen bonds.

Conclusions

In this study, we found that the combination of observation of the solid state ^{1}H NMR chemical shift and empirical chemical shift calculation was valid to characterize protons of silk I and silk II forms of the silk model peptide $(AG)_{15}$, especially for H^N. In the H^N region of silk I, Ala and Gly signals resonated separately, and they were assigned correctly by chemical shift calculations, by reference to ^{1}H−^{15}N 2D HETCOR measurements. Examination of the origin of the calculated chemical shift revealed that the chemical shift difference between Ala H^N in silk I and in silk II was predominantly due to a high-field shift in silk I arising from the magnetic anisotropy effect of the C−N bond of the preceding residue and a low-field shift in silk II arising from the magnetic anisotropy effect of the hydrogen bonding C═O bond. This result shows that we could distinguish proton chemical shift effects arising from intermolecular interactions from those arising from intramolecular interactions by combining observation of the solid state ^{1}H NMR chemical shift and empirical chemical shift calculations. Such observations are not possible for ^{13}C shifts. In summary, a combination of measurement of ^{1}H chemical shift with the information available from empirical chemical shift calculations can be regarded as a useful technique for molecular structure analysis by solid state

NMR, which otherwise has limited information content due to its having a lower resolution than solution NMR.

Acknowledgment. TA acknowledges support from the Grant-in-Aid for Scientific Research from the Ministry of Education, Science, Culture and Sports of Japan (18105007) and the Programme for Promotion of Basic and Applied Researches for Innovations in Bio-oriented Industry. Y.S. is grateful for the financial support provided by the Ministry of Education, Science, Sports, Culture and Technology for the support program for improving graduate school education of "Human Resource Development Program for Scientific Powerhouse" conducted in the Tokyo University of Agriculture & Technology. We thank Dr. Kenzo Deguchi at NIMS for NMR measurements and useful suggestions.

References and Notes

(1) Kishi, S.; Santos, A.; Ishii, O.; Ishikawa, K.; Kunieda, S.; Kimura, H.; Shoji, A. *J. Mol. Struct.* **2003**, *649*, 155.
(2) Shoji, A.; Kimura, H.; Sugisawa, H. *Annu. Rep. NMR Spectrosc.* **2002**, *45*, 69.
(3) Wei, Y. F.; Lee, D. K.; Hallock, K. J.; Ramamoorthy, A. *Chem. Phys. Lett.* **2002**, *351*, 42.
(4) Samoson, A.; Tuherm, T.; Gan, Z. *Solid State Nucl. Magn. Reson.* **2001**, *20*, 130.
(5) Schnell, I.; Spiess, H. W. *J. Magn. Reson.* **2001**, *151*, 153.
(6) Suzuki, Y.; Okonogi, M.; Yamauchi, K.; Kurosu, H.; Tansho, M.; Shimizu, T.; Saito, H.; Asakura, T. *J. Phys. Chem. B* **2007**, *111*, 9172.
(7) Yamauchi, K.; Kuroki, S.; Fujii, K.; Ando, I. *Chem. Phys. Lett.* **2000**, *324*, 435.
(8) Nevzorov, A. A.; Park, S. H.; Opella, S. J. *J. Biomol. NMR* **2007**, *37*, 113.
(9) Oldfield, E. *J. Biomol. NMR* **1995**, *5*, 217.
(10) Xu, X. P.; Case, D. A. *Biopolymers* **2002**, *65*, 408.
(11) Williamson, M. P.; Asakura, T. *J. Magn. Reson. B* **1993**, *101*, 63.
(12) Asakura, T.; Taoka, K.; Demura, M.; Williamson, M. P. *J. Biomol. NMR* **1995**, *6*, 227.
(13) Sitkoff, D.; Case, D. A. *Prog. Nucl. Magn. Reson. Spectrosc.* **1998**, *32*, 165.
(14) Moon, S.; Case, D. A. *J. Biomol. NMR* **2007**, *38*, 139.
(15) Neal, S.; Nip, A. M.; Zhang, H. Y.; Wishart, D. S. *J. Biomol. NMR* **2003**, *26*, 215.
(16) Refaee, M.; Tezuka, T.; Akasaka, K.; Williamson, M. P. *J. Mol. Biol.* **2003**, *327*, 857.
(17) Williamson, M. P.; Akasaka, K.; Refaee, M. *Protein Sci.* **2003**, *12*, 1971.
(18) Wilton, D. J.; Tunnicliffe, R. B.; Kamatari, Y. O.; Akasaka, K.; Williamson, M. P. *Proteins: Struct., Funct., Bioinf.* **2008**, *71*, 1432.
(19) Williamson, M. P.; Kikuchi, J.; Asakura, T. *J. Mol. Biol.* **1995**, *247*, 541.
(20) Cavalli, A.; Salvatella, X.; Dobson, C. M.; Vendruscolo, M. *Proc. Natl. Acad. Sci. U.S.A.* **2007**, *104*, 9615.
(21) Shen, Y.; Lange, O.; Delaglio, F.; Rossi, P.; Aramini, J. M.; Liu, G. H.; Eletsky, A.; Wu, Y. B.; Singarapu, K. K.; Lemak, A.; Ignatchenko, A.; Arrowsmith, C. H.; Szyperski, T.; Montelione, G. T.; Baker, D.; Bax, A. *Proc. Natl. Acad. Sci. U.S.A.* **2008**, *105*, 4685.
(22) Asakura, T.; Ashida, J.; Yamane, T.; Kameda, T.; Nakazawa, Y.; Ohgo, K.; Komatsu, K. *J. Mol. Biol.* **2001**, *306*, 291.
(23) Asakura, T.; Yamane, T.; Nakazawa, Y.; Kameda, T.; Ando, K. *Biopolymers* **2001**, *58*, 521.
(24) Gullion, T.; Kishore, R.; Asakura, T. *J. Am. Chem. Soc.* **2003**, *125*, 7510.
(25) Asakura, T.; Ohgo, K.; Komatsu, K.; Kanenari, M.; Okuyama, K. *Macromolecules* **2005**, *38*, 7397.
(26) Okuyama, K.; Somashekar, R.; Noguchi, K.; Ichimura, S. *Biopolymers* **2001**, *59*, 310.
(27) Lotz, B.; Keith, H. D. *J. Mol. Biol.* **1971**, *61*, 195.
(28) Asakura, T.; Yao, J.; Yamane, T.; Umemura, K.; Ulrich, A. S. *J. Am. Chem. Soc.* **2002**, *124*, 8794.
(29) Kameda, T.; Nakazawa, Y.; Kazuhara, J.; Yamane, T.; Asakura, T. *Biopolymers* **2002**, *64*, 80.
(30) Asakura, T.; Sato, H.; Moro, F.; Yang, M. Y.; Nakazawa, Y.; Collins, A. M.; Knight, D. *Macromolecules* **2007**, *40*, 8983.
(31) Asakura, T.; Nakazawa, Y.; Ohnishi, E.; Moro, F. *Protein Sci.* **2005**, *14*, 2654.
(32) Lotz, B.; Cesari, F. C. *Biochimie* **1979**, *61*, 205.
(33) Fossey, S. A.; Nemethy, G.; Gibson, K. D.; Scheraga, H. A. *Biopolymers* **1991**, *31*, 1529.
(34) Takahashi, Y.; Gehoh, M.; Yuzuriha, K. *Int. J. Biol. Macromol.* **1999**, *24*, 127.
(35) Tanaka, C.; Asakura, T. *Biomacromolecules* **2009**, *10*, 923.
(36) Nakazawa, Y.; Asakura, T. *J. Am. Chem. Soc.* **2003**, *125*, 7230.
(37) Lee, D. K.; Ramamoorthy, A. *J. Phys. Chem. B* **1999**, *103*, 271.
(38) Wildman, K. A. H.; Wilson, E. E.; Lee, D. K.; Ramamoorthy, A. *Solid State Nucl. Magn. Reson.* **2003**, *24*, 94.
(39) Tanaka, C.; Takahashi, R.; Asano, A.; Kurotsu, T.; Akai, H.; Sato, K.; Knight, D. P.; Asakura, T. *Macromolecules* **2008**, *41*, 796.
(40) Asakura, T.; Kuzuhara, A.; Tabeta, R.; Saito, H. *Macromolecules* **1985**, *18*, 1841.
(41) Saito, H.; Tabeta, R.; Asakura, T.; Iwanaga, Y.; Shoji, A.; Ozaki, T.; Ando, I. *Macromolecules* **1984**, *17*, 1405.
(42) Vinogradov, E.; Madhu, P. K.; Vega, S. *Chem. Phys. Lett.* **1999**, *314*, 443.
(43) Lee, M.; Goldburg, W. I. *Phy. Rev. A* **1965**, *140*, 1261.
(44) Asakura, T.; Demura, M.; Date, T.; Miyashita, N.; Ogawa, K.; Williamson, M. P. *Biopolymers* **1997**, *41*, 193.
(45) Williamson, M. P. *Biopolymers* **1990**, *29*, 1428.
(46) ApSimon, J. W.; Craig, W. G.; Demarco, P. V.; Mathieson, D. W.; Saunders, L.; Whalley, W. B. *Tetrahedron* **1967**, *23*, 2357.
(47) ApSimon, J. W.; Demarco, P. V.; Mathieso, D. W. *Tetrahedron* **1970**, *26*, 119.
(48) Blanchard, L.; Hunter, C. N.; Williamson, M. P. *J. Biomol. NMR* **1997**, *9*, 389.
(49) Iwadate, M.; Asakura, T.; Williamson, M. P. *J. Biomol. NMR* **1999**, *13*, 199.

JP903020P